# Preparation of Lignin-like Polymers by Dehydrogenation of Lignin Precursors and Structure-activity Relationships of the Resulting Polymers against Live Cancer HepG2 Cells

Boxuan Zhao, a Zhijian Li, b, Zhi Wang, Yunbo Zhao, and Yimin Xie a, c, \*

Lignin can be used as a natural anticancer drug because of its potential biological activity and low cytotoxicity. This research focuses on oligomeric dehydrogenation polymers (DHPs) of lignin. The lignin precursor coniferin was used to yield Zulaufverfahren dehydrogenation polymers (ZL-DHPs) and Zutropfverfahren dehydropolymers (ZT-DHPs) catalyzed by mixed enzymes. The <sup>13</sup>C-NMR determination showed that the DHPs obtained were similar to natural lignin, and ZL-DHP had a slightly higher  $\beta$ -5 content than ZT-DHP. ZL-DHPs and ZT-DHPs were subjected to organic solvent extraction with different polarities to obtain eight fractions, i.e., ZL-1-ZL-4 and ZT-1-ZT-4. The antitumor activity showed ZL-2 (IC<sub>50</sub> 181.99 µg/mL) and ZT-2 (IC<sub>50</sub> 246.76 µg/mL) had significant inhibitory effects. Fractions ZL-2 and ZT-2 were purified through column chromatography using gradient-polarity binary eluent, and 12 purified compounds were obtained, i.e., L1-L6 and T1-T6. The results showed L2 (IC<sub>50</sub> 33.99 µg/mL) and T1  $(IC_{50}42.08 \mu g/mL)$  had relatively high biological activity, respectively. Their structure was characterized using high-resolution mass spectrometry and <sup>13</sup>C-NMR, indicating that L2 is a dimer with  $\beta$ -5 linkage ( $\beta$ -5,  $\gamma$ -CH<sub>3</sub>, and  $\gamma'$ -CH<sub>2</sub>OH), and T1 is also a dimer with  $\beta$ -5 linkage but different substituents ( $\beta$ -5,  $\gamma$ -CHO, and  $\gamma$ '-COOH).

DOI: 10.15376/biores.20.2.2904-2921

Keywords: Lignin; Dehydrogenation polymers; Anticancer; Mass spectrometry; Structure-activity relationship

Contact information: a: Research Institute of Pulp & Paper Engineering, Hubei University of Technology, Wuhan 430068 China; b: Wuhan Children's Hospital (Wuhan Maternal and Child Health Hospital, Wuhan Women's and Children's Health Care Center), No.100 Xianggang Road, Wuhan, 430000 China; 64473787@qq.com (Z.L.); c: Hubei Provincial Key Laboratory of Green Materials for Light Industry, Hubei University of Technology, Wuhan 430068 China; ppymxie@l63.com

#### INTRODUCTION

The use of lignin oligomers, such as dimers or trimers, to investigate the bioreactivity of natural lignin has become a promising research area. The most common method for preparing oligomeric dehydrogenation polymers (DHPs) involves the use of horseradish peroxidase (HRP) and hydrogen peroxide to dehydrogenation polymerize monolignols in a buffer (Freudenberg 1965; Tobimatsu *et al.* 2006). This process simulates the biosynthesis of natural lignin and provides a powerful tool for lignin research. Currently, two polymerization methods, *i.e.*, *Zulaufverfahren* (ZL) and *Zutropfverfahren* (ZT), are used (Cathala and Monties 2001). *Zulaufverfahren* involves bulk polymerization of monolignols by flow addition; however, its dimer products are abundant compared to

natural lignin. *Zutropfverfahren* involves a slow drop-wise addition of a mixed solution of the reaction substrate and hydrogen peroxide into a buffer containing HRP, which helps simulate the terminal polymerization process during lignification and reduces the proportion of dimerization products. However, compared with the *Zulaufverfahren* method, the *Zutropfverfahren* method produces DHPs with a physiological activity more similar to that of native lignin (Johjima *et al.* 1999; Méchin *et al.* 2007).

Lignin dehydrogenated polymers also show significant potential for applications in anticancer research. It has been reported that the DHPs synthesized from coniferin and purified using organic solvents inhibit HeLa cervical cancer cells and A549 lung cancer cells (Chen 2019; Wei 2022; Zhou *et al.* 2023). These oligomeric lignins provide a powerful tool for understanding the mechanism underlying their effect on cancer cells. Chen *et al.* (2019) revealed the contributions of different structural units to the biological activity of guaiacyl-type oligomeric lignin (DHP-G) and guaiacyl-syringyl-type DHP (DHP-GS) derived from coniferin and syringin. The results showed that the  $\beta$ -O-4 structure does not contribute to the biological activity of DHP, whereas the  $\beta$ -5 structure increases the inhibitory effect of DHP on cervical cancer HeLa cells. Wei (2022) further compared the inhibitory effects of DHP with those of purified compounds isolated from ginkgo kraft lignin on A549 lung cancer cells and found that an increase in the aldehyde group on the side chain of the phenylpropane unit can enhance antitumor activity. These studies have provided preliminary results in understanding the antitumor activity of oligomeric lignin derivatives (Shu *et al.* 2021).

Liver cancer is the third most common malignant tumor, after gastric and esophageal cancers (Anwanwan *et al.* 2020). Therefore, novel anticancer drugs are required. In the present study, coniferin was used as the starting material, and with HRP,  $\beta$ -glucosidase, and glucose oxidase as catalysts, the oligomeric lignin fractions were obtained using the *Zulaufverfahren* (ZL) and *Zutropfverfahren* (ZT) methods followed by fractionation and purification. The inhibitory effect of each fraction on HepG2 cells was evaluated using the 3-[4,5-dimethylthiazol-2-yl]-2,5 diphenyl tetrazolium bromide (MTT) assay (Van Meerloo *et al.* 2011; Kumar *et al.* 2018). Fractions with higher biological activity were further purified through column chromatography using a polar solvent gradient. The purified compounds were subjected to the above-mentioned biological activity determinations (Ugartondo *et al.* 2008; Zhao *et al.* 2017). In addition, the structure was analyzed to reveal the possible mechanism underlying the anti-hepatoma activity of lignin and to understand the structure-effect relationship.

#### **EXPERIMENTAL**

#### **Materials**

Phosphate buffer saline (PBS) was purchased from Gibco (Grand Island, NY, USA). HRP,  $\beta$ -glucosidase, and glucose oxidase were purchased from Sigma-Aldrich (St. Louis, MO, USA). Complete EMEM (containing penicillin-streptomycin) and fetal bovine serum were obtained from Wuhan Boster Bioengineering Co., Ltd (International Enterprise Center, 1 Te 1, Guanshan 2<sup>nd</sup> Road, Wuhan). MTT cells were obtained from Beijing Lanjie Technology Co., Ltd. (Room 206, Building 1, 9 Yumin Avenue, Area B, Konggang Industrial Park, Shunyi District, Beijing), and liver cancer HepG2 cells were purchased from Beijing Beina Biotechnology Co., Ltd. (Building 5A, Shuanghuiyuan, Chaoyang District, Beijing). Coniferin was synthesized in the laboratory.

#### **Biosynthesis of ZL-DHP**

Coniferin (500 mg) was dissolved in a 250 mL three-neck bottle flask with 50 mL of 0.2 M sterile acetic acid/sodium acetate buffer solution at pH 5.0. After the system was stabilized, glucose oxidase,  $\beta$ -glucosidase, and HRP were added. Sterile air filtered through activated carbon was continuously bubbled, and the reaction was conducted at 30 °C for 9 h. Then, glucose oxidase,  $\beta$ -glucosidase, and HRP were supplemented, and the reaction was continued for 87 h. Then, 150 mL of distilled water was added and the mixture was heated to 65 °C to stop the reaction. The mixture was centrifuged, and the precipitate was collected and washed three times with distilled water to remove the soluble enzymes. Crude ZL-DHP was obtained by freeze drying, and dissolved in dichloroethane/ethanol (2:1/v:v), extracted for 4 h, and centrifuged. The supernatant was collected and vacuum-dried- to obtain purified ZL-DHP with a yield of 41.9%.

#### **Biosynthesis of ZT-DHP**

Coniferin (500 mg) was dissolved in a 50 mL-erlenmeyer flask with 30 mL of 0.2 M sterile acetic acid/sodium acetate buffer solution at pH 5.0. Glucose oxidase,  $\beta$ -glucosidase, and HRP were dissolved in a 250 mL three-neck bottle flask with 20 mL of 0.2 M sterile acetic acid/sodium acetate buffer solution under sterile conditions. The coniferin solution was slowly added to the mixed enzyme solution by a constant current pump within 24 h at 30 °C. Glucose oxidase,  $\beta$ -glucosidase, and HRP were added to continue the reaction for 72 h. Then, 150 mL of distilled water was added and the mixture was heated to 65 °C to stop the reaction. The reaction mixture was centrifuged, and the precipitate was collected and washed three times with distilled water to remove the soluble enzymes. Crude ZT-DHP was obtained by freeze-drying, dissolved in dichloroethane/ethanol (v:v/2:1), and centrifuged. The supernatant was vacuum-dried to obtain purified ZT-DHP with a yield of 43.3%. The synthesis routes of the DHPs (ZL-DHP and ZT-DHP) are shown in Fig. 1 (Terashima *et al.* 1995, 1996).

Fig. 1. The structural changes of coniferin during the synthesis of DHPs

#### **ZL-DHP and ZT-DHP Fractionation**

According to the solubilities of DHPs in different polar organic solvents, cyclohexane, ethyl ether, ethanol, and dioxane were used to fractionate DHPs (Zega *et al.* 2008; Mattinen *et al.* 2011). The fractionation process is illustrated in Fig. 2. The DHP

fractions were first extracted with cyclohexane using a Soxhlet extractor (De Castro and Priego-Capote 2010), and the solvent was removed *in vacuo* to obtain the cyclohexane-soluble fraction, ZL-1/ZT-1. The residual solid was extracted with absolute ethyl ether using a Soxhlet extractor, and then it was extracted with ethanol and dioxane. Ethyl ether-soluble fraction ZL-2/ZT-2, ethanol-soluble fraction ZL-3/ZT-3, and dioxane-soluble fraction ZL-4/ZT-4 were obtained. The yields of ZL-1/ZT-1, ZL-2/ZT-2, ZL-3/ZT-3, ZL-4/ZT-4 were 3.8%/4.0%, 10.2%/10.0%, 43.1%/41.2%, 31.6%/32.6%, respectively.

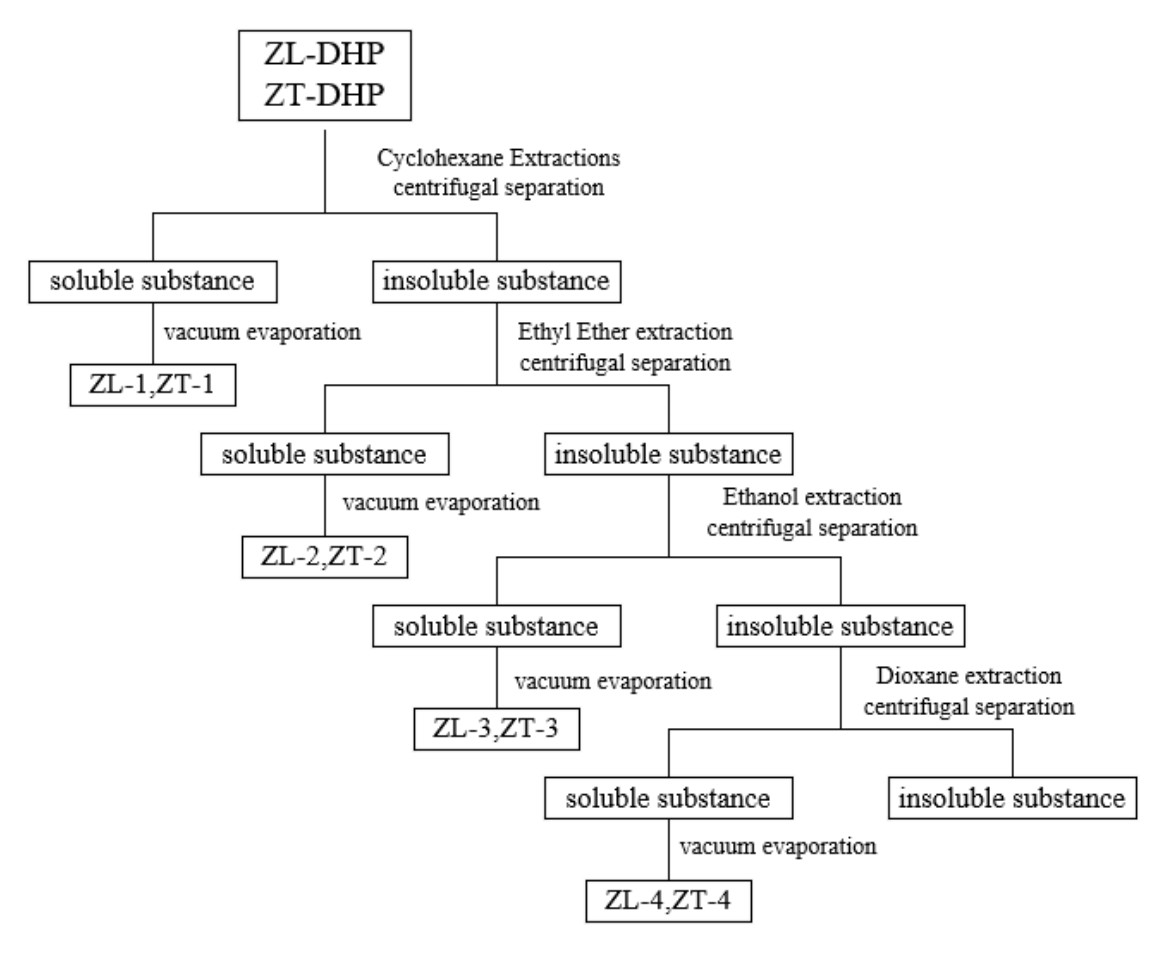


Fig. 2. Fractionation of ZL-DHP and ZT-DHP

#### Purification of the DHP Ether-soluble Fraction

Among the ZL-DHP and ZT-DHP fractions, the ether-soluble fraction, ZL-2/ZL-2, had the best biological activity. Therefore, these two fractions were further purified through column chromatography. A binary mixed solvent with gradient polarity was used as the eluent, and the process is shown in Fig. 3. Using cyclohexane-ethyl: acetate (v/v,4:1), cycloethane: ethanol (v/v, 1:1), dichloromethane: methanol (v/v, 9:1), ethyl acetate: ethanol (v/v, 5:1), ethyl acetate: methanol (v/v, 9:1), and chloroform: methanol (v/v, 9:1), the fractions ZL-2 and ZT-2 were eluted. The eluent was verified using TLC (Wang *et al.* 2006; Bele and Khale 2011). The highly consistent eluents were combined, and the solvent was evaporated under reduced pressure to obtain 12 groups of purified compounds. The yields of L1–L6 were 38.57%, 35.42%, 7.79%, 1.10%, 1.26%, and 7.24%, respectively. The yields of T1-T6 were 28.72%, 25.06%, 11.28%, 2.11%, 4.23%, and 23.24%, respectively.

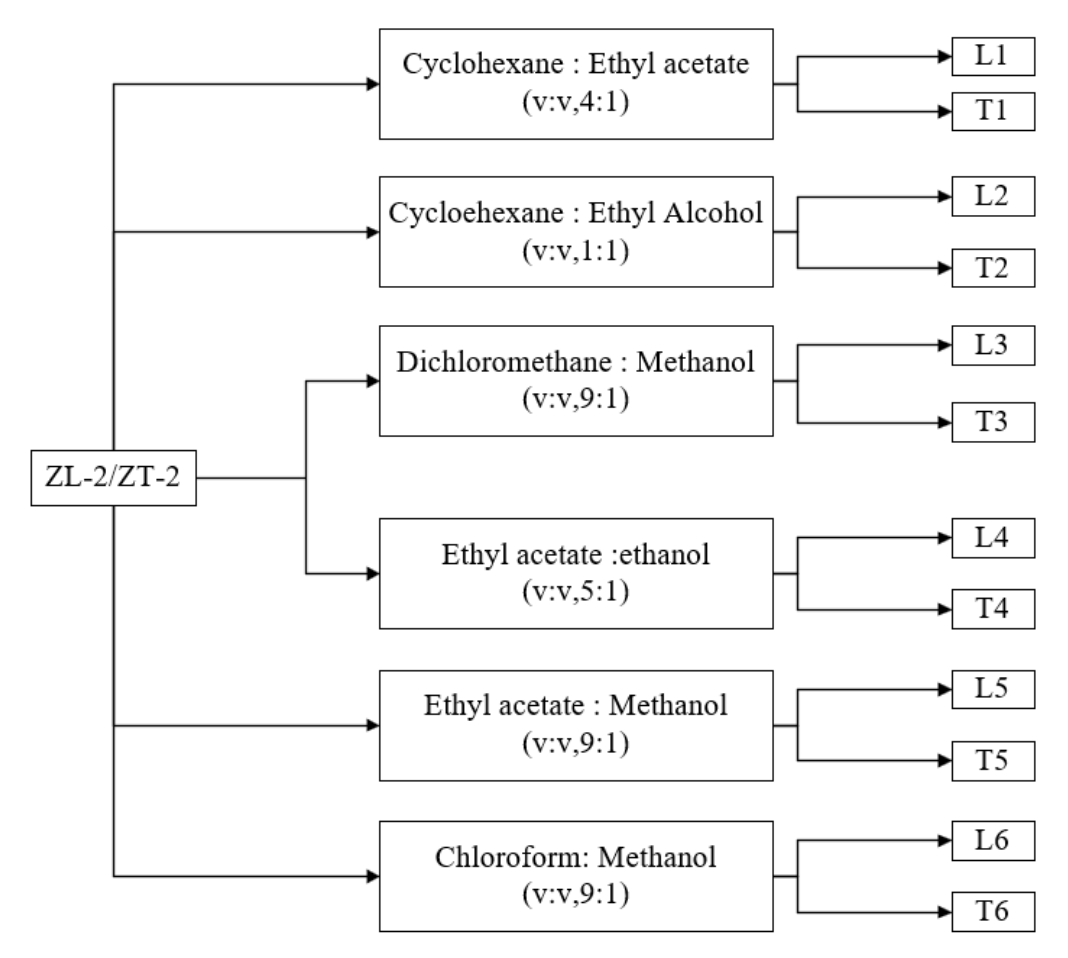


Fig. 3. Purification process of fraction ZL-2 and ZT-2 of DHPs

#### **Antitumor Activity Determination**

The MTT assay is commonly used to evaluate the antitumor activity of compounds against tumor cells (Ahamed et al. 2013). Each well of a 96-well plate was filled with sterile PBS and transferred to a cell culture chamber for 24 to 48 h. Once the bottom of the well was covered with cells, 100 µL of the sample solution, prepared at a gradient concentration, was dispensed into the experimental well. Then, the same solvent and complete medium were added to the control well, and the zero well was continuously supplemented with complete medium. The cells on the 96-well plate were incubated, and their cell growth was observed at regular intervals. After culturing for two days, the MTT solution (5 mg/mL) was added to the wells corresponding to the experimental, control, and zero groups and placed in an incubator. Four hours later, the spent medium in the well was discarded using a sterile syringe, and purple crystals formed. Dimethyl sulfoxide (DMSO, 150 µL) was added to each well, the plate was shaken in a microplate reader for 10 min, and the absorbance (OD) was measured at 490 nm. The OD of the test well was recorded as OD<sub>1</sub>, that of the control as OD<sub>2</sub>, and that of the zero well as OD<sub>3</sub>. The extent of inhibition of the samples at different concentrations were calculated according to Eq. 1, and the semiinhibitory concentration (IC<sub>50</sub>) of each sample was calculated using SPSS software (Nga et al. 2020). The concentration of the sample to be tested in the experimental group was set to 12.5 to 800 µg/mL using the double-dilution method. The sample was dissolved in 1 mL of complete medium. If the solubility was poor, an appropriate amount of organic

solvent, such as acetone, or the surfactant polysorbate 80 (0.5% Tween 80), was added first, followed by the addition of 1 mL complete medium.

Extent of inhibition(IR%)= 
$$\left(1 - \frac{\text{OD}_1 - \text{OD}_3}{\text{OD}_2 - \text{OD}_3}\right) \times 100$$
 (1)

## HRMS Mass Spectrometry Determination of Biologically Active Purified Components

The mass spectrometry information of L2 and T1 was obtained using the Q Exactive electrostatic field orbital ion well mass spectrometer (Thermo Fisher Scientific Inc., Waltham, MA, USA) (Nolting and Malek 2019). The parameters were as follows: ion source, HESI; dry gas,  $N_2$ ; atomizing gas pressure, 40 arb; auxiliary gas pressure, 10 arb; spray voltage, 3500 V; ion transport capillary temperature, 350 °C; scanning mode, negative ion full MS; scanning range m/z, 50 to 500.

#### <sup>13</sup>C-NMR Determination of ZL-DHP and ZT-DHP

ZL-DHP and ZT-DHP (40 mg) were dissolved in 0.6 mL DMSO- $d_6$ , and placed in a  $^{\oplus}$ 5-mm nuclear magnetic tube. The corresponding  $^{13}$ C-NMR spectra were obtained using a Bruker Avance III 600 MHz NMR spectrometer (8th Floor, Tower C, Building B-6, Zhongguancun Dongsheng Science and Technology Park, 66 Xixiaokou Road, Haidian District, Beijing) at 150.90 MHz. The parameters were as follows: test temperature, 22  $^{\circ}$ C; pulse delay, 2.0 s; acquisition time, 0.81 s; number of scans, 3000 times.

#### RESULTS AND DISCUSSION

#### Antitumor Activities of ZL-DHP and ZT-DHP

The relationships between the concentration and extent of inhibition of different ZL-DHP and ZT-DHP fractions obtained using solvent extraction on HepG2 hepatocellular carcinoma cells are shown in Fig. 4.

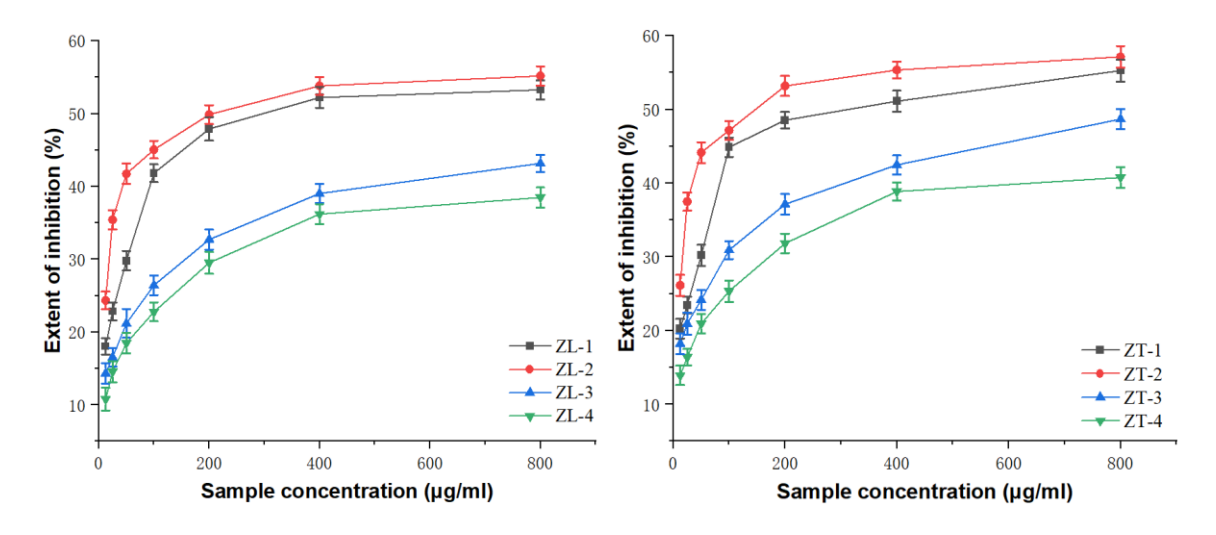


Fig. 4. Relationship of concentration of ZL-DHP (A) and ZT-DHP (B) fractions with the extent of inhibition of liver cancer HepG2 cells

All IC<sub>50</sub> calculated using the SPSS 26 software are shown in Table 1. All DHP fractions exhibited different degrees of inhibition on HepG2 hepatocellular carcinoma cells (Zhang *et al.* 2016). Among them, the ether-soluble fraction ZL-2/ZT-2 showed the best antitumor effect. The antitumor effect of the DHP fractions exhibited nonlinear doseresponse relationships over a range of concentrations. The ether-soluble fractions ZL-2/ZT-2 from ZL-DHP and ZT-DHP, had the lowest IC<sub>50</sub>, *i.e.*, 181.99 μg/mL and 246.76 μg/mL, respectively, demonstrating a stronger inhibitory effect on tumor cells (Table 1).

**Table 1.** Semi-inhibitory Concentration (IC<sub>50</sub>) of DHPs Fractions on Liver Cancer HepG2 Cells

DHPs graded fractions	IC <sub>50</sub> (μg/mL)
ZL-1	325.0
ZL-2	182.0
ZL-3	924.0
ZL-4	1729.3
ZT-1	340.3
ZT-2	246.8
ZT-3	1435.6
ZT-4	2011.6

#### <sup>13</sup>C-NMR analyses of ZL-DHP and ZT-DHP

The <sup>13</sup>C-NMR spectra of ZL-DHP and ZT-DHP are shown in Fig. 5. The <sup>13</sup>C-NMR spectra revealed clear differences in the chemical structures of ZL-DHP and ZT-DHP. Both DHPs had signals near 194.7 ppm (No. 1), which correspond to the  $\gamma$ -CHO of cinnamaldehyde, indicating that oxidation occurred during coniferin polymerization. A signal near 172.7 ppm (No. 2) corresponds to the  $\gamma$ -position of the ferulic acid unit, indicating that the hydroxymethyl group at the  $\gamma$ -position was oxidized to a carboxyl group. The signals at 150.3 to 131.3 ppm (Nos. 4–8) were mainly from the carbon atoms on the guaiacyl aromatic ring. Signals at 129.6 ppm (No. 9) and 129.5 ppm (No. 10) are caused by the resonance of  $C\alpha$  and  $C\beta$  in the structure of coniferyl alcohol. This reveled that both DHPs prepared by the bulk and the end-wise methods contained a part of the  $C\alpha H = C\beta H$ structure, which is consistent with previous results (Xie et al. 1994). The resonance signals in the 119.4 to 110.7 ppm (Nos. 13–16) region are all from carbon atoms on the aromatic ring. The signals near 87.5 to 85.4 ppm correspond to the  $\beta$ -5 (No. 17) and C $\beta$  in  $\beta$ -O-4 structures and  $C\alpha$  in  $\beta$ - $\beta$  (No. 18). The signals in the 74.2 to 70.6 ppm (Nos. 20–22) region and 62.1 ppm (No. 25) correspond to  $C\alpha$  and  $C\gamma$  in the  $\beta$ -O-4 structure, and 67.7 ppm (No. 23) and 53.7 ppm (No. 27) arise from C $\beta$  and C $\gamma$  in the  $\beta$ -5 structure, respectively. The signals at 63.4 ppm (No. 24) and 47.0 ppm (No. 28) are from C $\alpha$  in the  $\beta$ -1 structure and  $C\beta$  in the  $\beta$ - $\beta$  structure, respectively. These results indicate that the artificially synthesized DHPs mainly contain  $\beta$ -5 and  $\beta$ -O-4 structures, as well as  $\beta$ - $\beta$ ,  $\beta$ -1, and phenylpropane structures such as cinnamaldehyde and ferulic acid. From the peak intensity, ZL-DHP is rich in the  $\beta$ -5 structure. Based on careful analysis of the <sup>13</sup>C-NMR spectra, it is found that that the signals corresponding to positions No. 2 and No. 3 in ZT-DHP exhibit higher intensities compared to those in ZL-DHP. This difference in intensity is caused by the higher carboxyl group content present in ZT-DHP. Conversely, the signal peaks at No. 23 and No. 30 in ZL-DHP are stronger than those in ZT-DHP, indicating a higher abundance of CyH2OH and CH3 groups in ZL-DHP. The coniferyl alcohol CyH2OH structure is represented by the signal peak at No. 25.

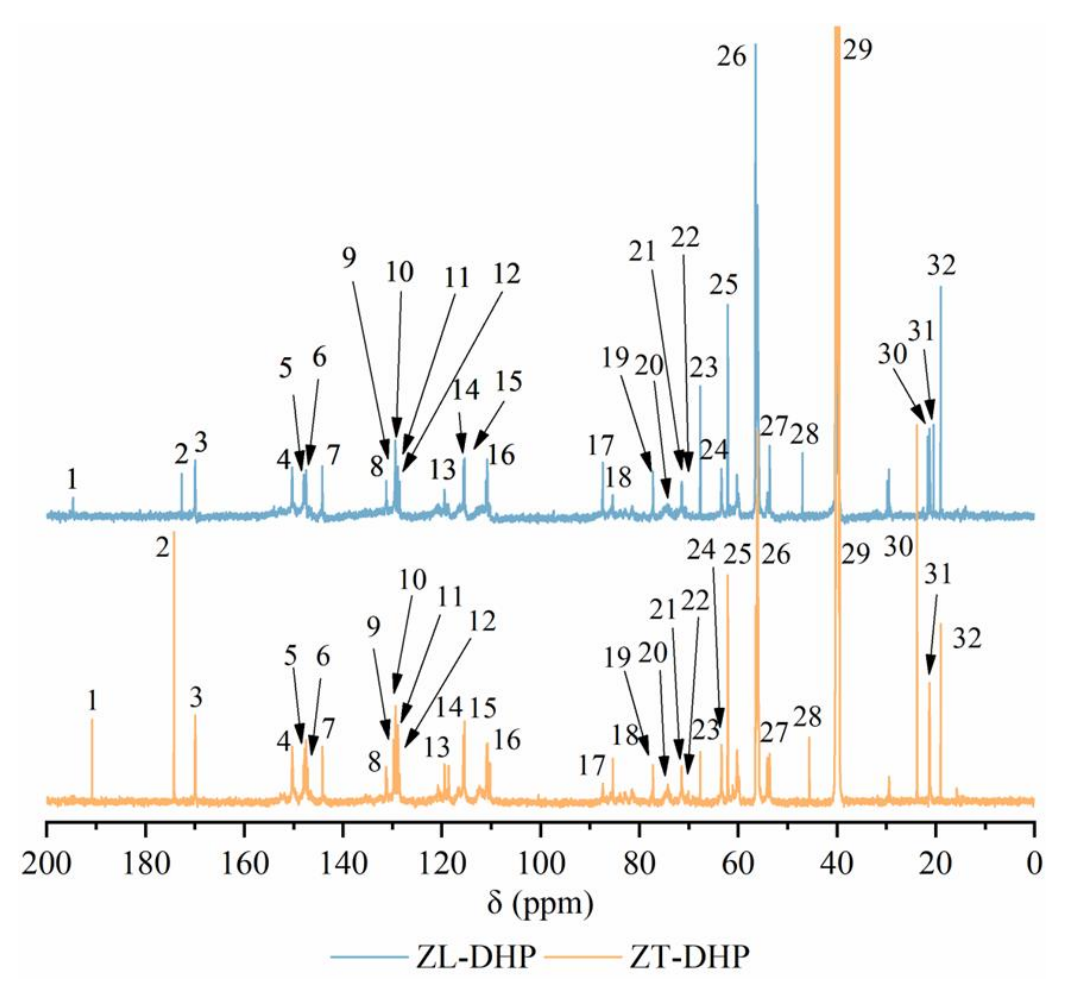
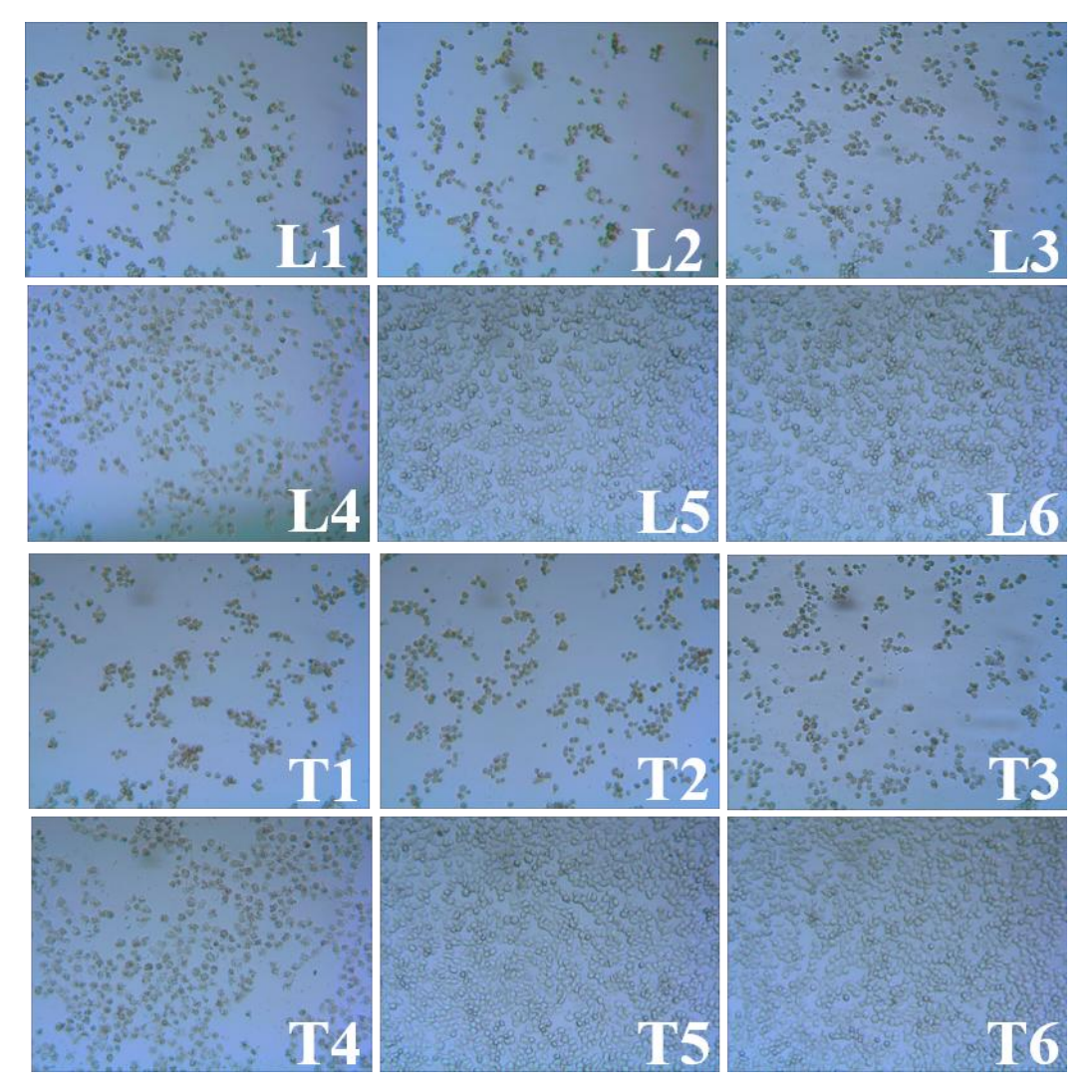


Fig. 5. <sup>13</sup>C-NMR spectra of ZL-DHP and ZT-DHP

#### Analyses of the Antitumor Activity of Purified DHP Compounds

The effect of the purified DHP compounds on the growth of HepG2 cells at the maximum concentration (800 µg/mL) is shown in Fig. 6. Each purified compound had an inhibitory effect on HepG2 liver cancer cells, especially the purified compounds L2 and T1. After adding the samples, the number of cells decreased significantly and the cells became small. This morphological change is consistent with the characteristics of cancer cell apoptosis, indicating that the purified compounds L2 and T1 have strong anticancer activity and can induce apoptosis of the cells (Liu *et al.* 2000; Park *et al.* 2014), thereby inhibiting the growth and proliferation of cancer cells.

The relationship between the extent of inhibition of purified DHPs on HepG2 cells is shown in Fig. 7. The IC $_{50}$  of each compound was calculated using SPSS 26 software, and the results are shown in Table 2 (Long *et al.* 2021). As shown in Fig. 7, compounds L2 and T1 had different degrees of inhibitory effect on HepG2 liver cancer cells, with a maximum extent of inhibition close to 80%. Among the purified DHP compounds, L2 and T1 had the better inhibitory effect on HepG2 cells, and their IC $_{50}$  values reached 34.0 and 42.1 µg/mL, respectively (Table 2). In general, the inhibitory effect of the compound purified from ZL-DHP on HepG2 cells was greater than that of the DHP synthesized using the end-wise method.



**Fig. 6.** Effect of purified compounds from DHPs on the growth status of liver cancer HepG2 cells at maximum concentrations

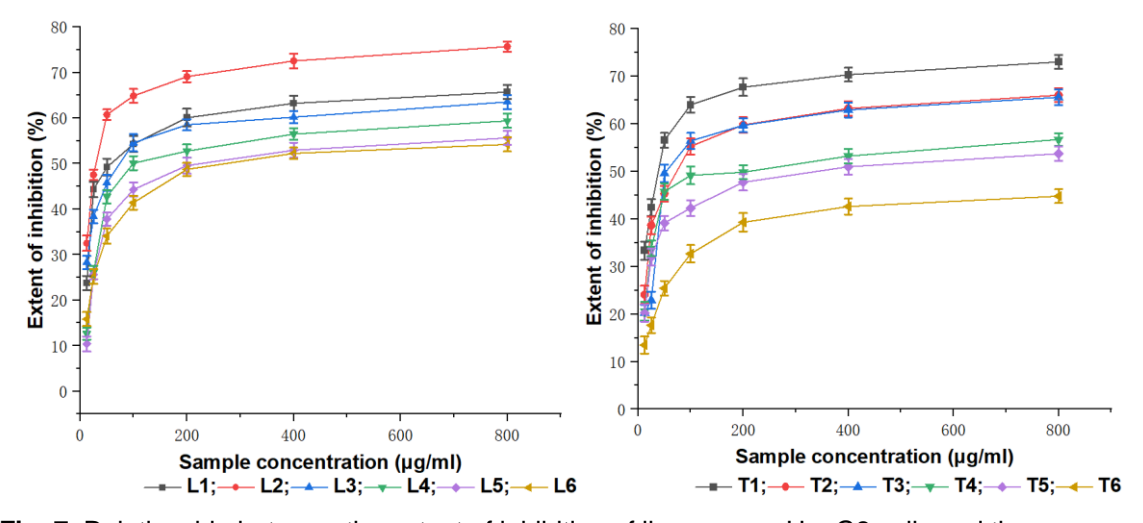


**Fig. 7.** Relationship between the extent of inhibition of liver cancer HepG2 cells and the concentrations of purified compounds from DHPs

**Table 2.** IC<sub>50</sub> of the Purified Compounds from DHPs on Liver Cancer HepG2 Cells

DHPs Purified compounds	IC <sub>50</sub> (μg/mL)
L1	84.0
L2	34.0
L3	101.2
L4	195.7
L5	276.7
L6	324.1
T1	42.1
T2	96.4
T3	138.3
T4	213.5
T5	332.3
T6	875.0

## HRMS Mass Spectrometry Analysis of the Biologically Active Purified Compounds

High-resolution mass spectrometry (HRMS) is an analytical technique that can distinguish between the molecular masses of compounds, provide high-resolution data (Zhang *et al.* 2021), and help to determine the structures and functional groups of compounds with high biological activity (Cui *et al.* 2021; Dean *et al.* 2022).

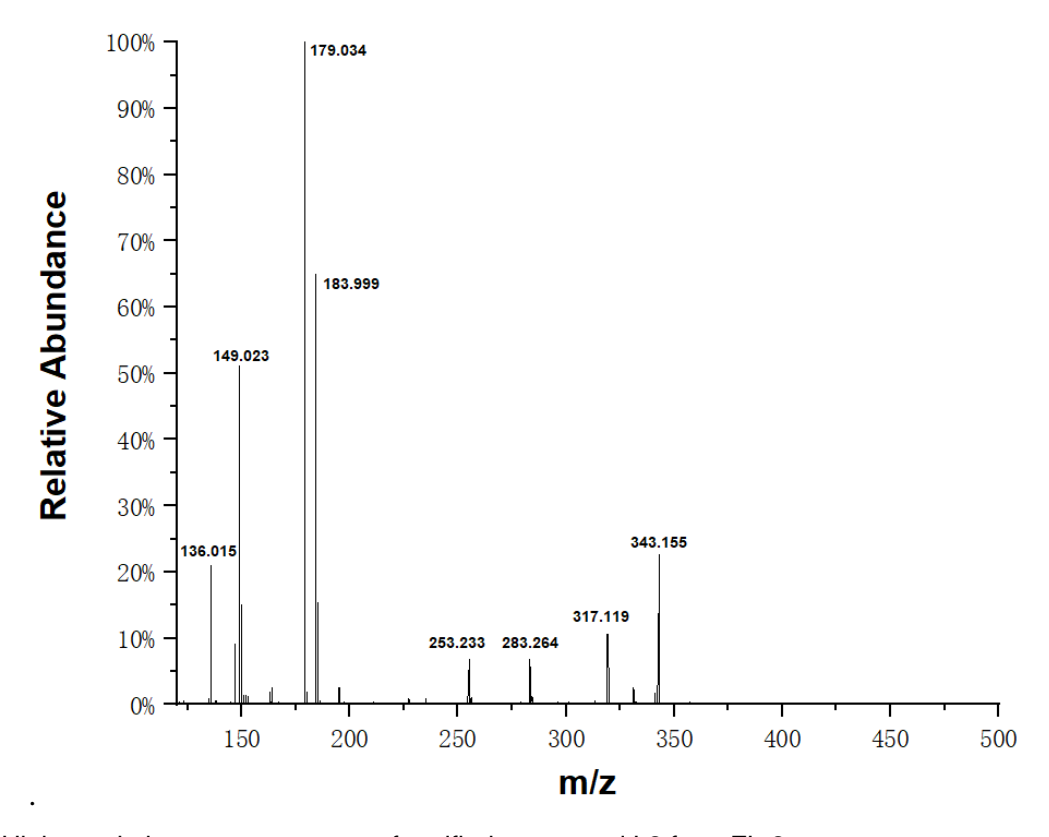


Fig. 8. High-resolution mass spectrum of purified compound L2 from ZL-2

**Table 3.** Fragment Information and Structure Determination of L2 Purified Compounds from ZL-2

m/z	Fragment assignment
136.015	Fragment assignment  OCH <sub>3</sub> OH  *H <sub>2</sub> C
149.023	OCH <sub>3</sub> OH
179.034	OCH <sub>3</sub>
183.999	OCH <sub>3</sub>
253.233	HOH <sub>2</sub> C COOH
283.264	OCH <sub>3</sub> OH OCH <sub>3</sub> OCH <sub>3</sub>
317.119	OCH <sub>3</sub> OCH <sub>3</sub> OCH <sub>3</sub> OCH <sub>3</sub> OCH <sub>3</sub>
343.155	HOH <sub>2</sub> C OCH <sub>3</sub> OCH <sub>3</sub>

Figure 8 shows the mass spectrum of L2, a compound purified from the ether-soluble fraction ZL-2 of ZL-DHP, which exhibits high biological activity. Table 3 shows the assignment of fragment ion peaks according to the spectrum. Among the various fragments, the prominent peak at m/z 179.034 corresponds to the ion signal of the coniferyl aldehyde monomer, whereas that at m/z 183.999 can be assigned to the coniferyl alcohol monomer. The peak at m/z 149.023, caused by the elimination of the  $\gamma$ -carbon in the coniferyl aldehyde side chain, implies the presence of 2-methoxy-4-vinyl phenol. Additionally, the elimination of  $\beta$  and  $\gamma$  carbons yields a fragment peak at m/z 136.015. Notably, the ion peak at m/z 343.155 represents a  $\beta$ -5 dimeric structure, formed via peroxidase-catalyzed coupling between a coniferyl aldehyde side chain double bond and phenolic hydroxyl group of another monomer (Matsushita et al. 2015; Xie et al. 2020).

Similarly, Fig. 9 shows the mass spectrum of T1, a compound purified from the diethyl ether-soluble ZT-2 fraction of ZT-DHP, characterized by its biological activity. The fragment information and assignments are summarized in Table 4. The molecular ion peak at m/z 371.186 corresponds to the molecular formula  $C_{20}H_{18}O_{7}$  for T1. The most abundant fragment ion peak at m/z 184.047 is hypothesized to be from a coniferyl alcohol monomer fragment (Liu *et al.* 2010; Takahashi *et al.* 2011). Similar to the L2, a notable peak at m/z 151.039 results from the cleavage of the coumaran structure, revealing the instability and eliminability of the  $C\gamma$  carbon of phenylpropane units. The ion peak at m/z 371.186 represents a dimer fragment with a  $\beta$ -5 linkage carrying oxidized side chains ( $\beta$ -5,  $\gamma$ -CHO, and  $\gamma$ '-COOH), indicating the occurrence of oxidation reactions. Fragmentation of this dimer into two ions at m/z 283.264 and m/z 325.144 confirms the presence of the  $\beta$ -5 characteristic structure.

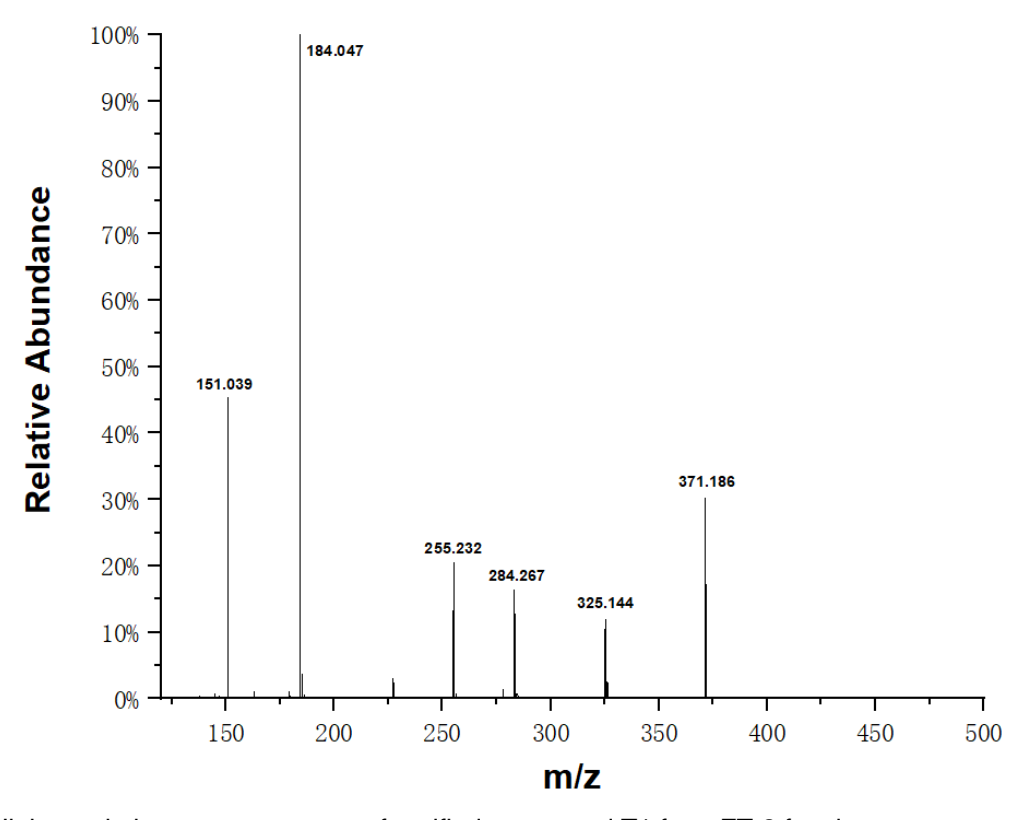


Fig. 9. High-resolution mass spectrum of purified compound T1 from ZT-2 fraction

**Table 4.** Fragment Information and Structural Assignment of Purified Compound T1 from ZT-2

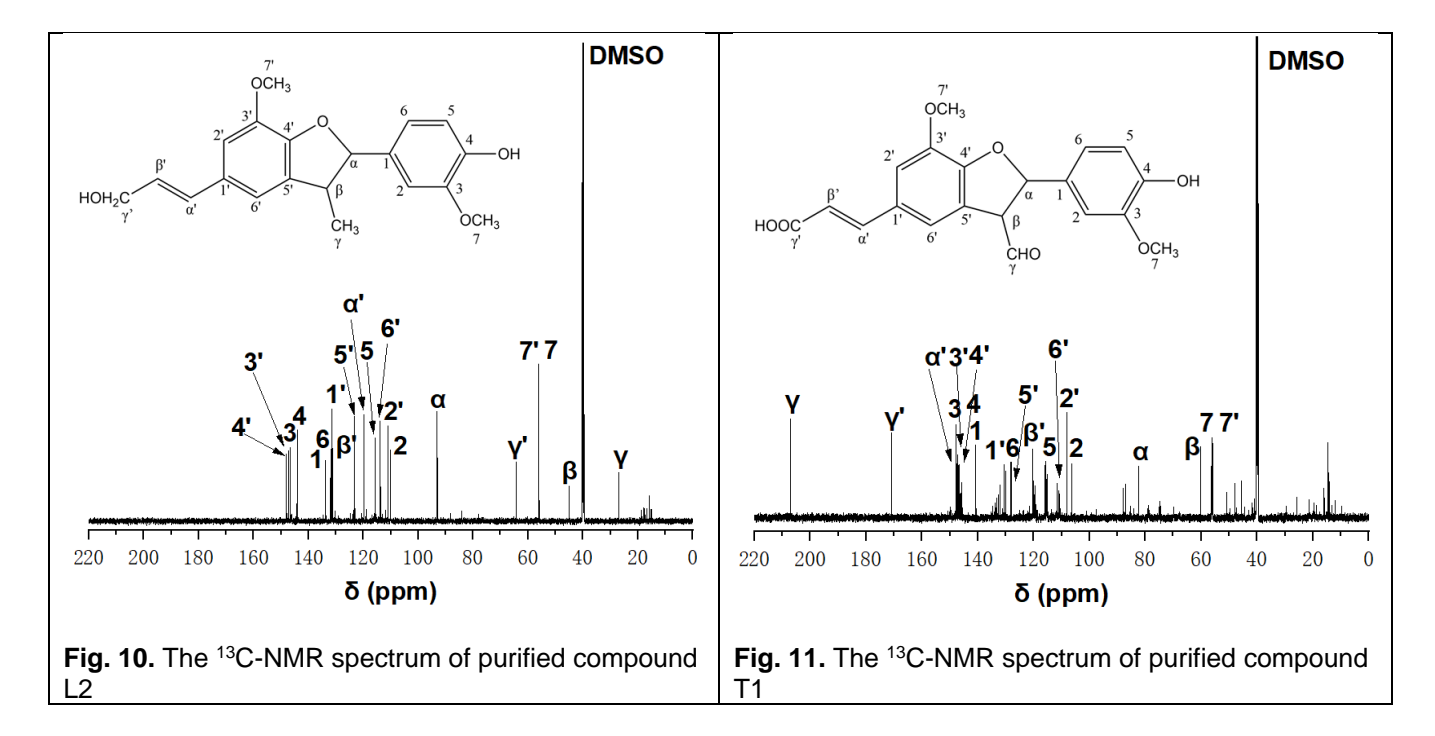
m/z	Structural assignment och <sub>3</sub>
151.039	*HC OH
184.047	OCH <sub>3</sub> OH HOH <sub>2</sub> C
255.232	OCH <sub>3</sub> OH CH <sub>2</sub> OH CH <sub>3</sub>
284.267	осн <sub>3</sub> осн <sub>3</sub> осн <sub>3</sub> осн <sub>3</sub>
325.144	OCH <sub>3</sub> OH OCH <sub>3</sub> OCH <sub>3</sub>
371.186	HOOC OCH <sub>3</sub> OCH <sub>3</sub> OCH <sub>3</sub>

### <sup>13</sup>C-NMR Analysis of the Purified Compounds with High Biological Activity

The  $^{13}$ C-NMR spectrum of L2 from ZL-DHP is shown in Fig. 10. The signals and their assignments are as follows:  $\delta 148.10$  (C4'),  $\delta 147.32$  (C3'),  $\delta 146.67$  (C3),  $\delta 144.13$  (C4),  $\delta 133.82$  (C1),  $\delta 131.83$  (C6),  $\delta 131.45$  (C1'),  $\delta 131.15$  (C $\beta$ ')  $\delta 123.15$  (C5'),  $\delta 119.81$  (C $\alpha$ '),  $\delta 115.70$  (C5).  $\delta 113.80$  (C6'),  $\delta 111.02$  (C2'),  $\delta 110.12$  (C2),  $\delta 93.07$  (C $\alpha$ ),  $\delta 64.18$  (C $\gamma$ '),  $\delta 56.12$  (C7'),  $\delta 56.08$  (C7),  $\delta 45.00$  (C $\beta$ ),  $\delta 39.80$  (DMSO-d $_6$  solvent), and  $\delta 26.81$  (C $\gamma$ ).

The  $^{13}$ C-NMR spectrum of T1 from ZT-DHP is shown in Fig. 11. The main signals and their assignments are as follows:  $\delta 206.99$  (C $\gamma$ ),  $\delta 170.82$  (C $\gamma$ '),  $\delta 147.99$  (C $\alpha$ '),  $\delta 147.93$  (C3),  $\delta 147.20$  (C3'),  $\delta 146.81$  (C4),  $\delta 145.85$  (C4 '),  $\delta 140.80$  (C1),  $\delta 130.48$  (C1'),  $\delta 129.96$  (C6),  $\delta 128.08$  (C5').  $\delta 120.44$  (C $\beta$ '),  $\delta 115.70$  (C5),  $\delta 111.10$  (C6'),  $\delta 108.20$  (C2'),  $\delta 106.26$ 

(C2),  $\delta 82.50$  (C $\alpha$ ),  $\delta 60.23$  (C $\beta$ ),  $\delta 56.16$  (C7),  $\delta 55.88$  (C7'), and  $\delta 40.21$  (DMSO).



According to the comprehensive analysis of the  $^{13}$ C-NMR and HRMS mass spectra of the purified compound L2 and T1 from the ether-soluble fraction ZL-2 and ZT-2 of DHPs, it can be concluded that the purified compounds of these two DHP samples are dimers with  $\beta$ -5 structures. The compound L2 is a  $\beta$ -5 structure ( $\beta$ -5,  $\gamma$ -CH<sub>3</sub>, and  $\gamma'$ -CH<sub>2</sub>OH) dimer, whereas T1 is a ( $\beta$ -5,  $\gamma$ -CHO, and  $\gamma'$ -COOH) dimer formed by coupling of side chain carbons and oxidation (Yue *et al.* 2016; Sheng *et al.* 2017).

#### Structure-activity Relationship of the Highly Bioactive Purified Compounds

Many studies have been conducted on the biological activity of lignin model compounds. Aljawish *et al.* (2014) synthesized a stable compound through laccase-catalyzed oxidation of ethyl ferulate and found that the dimer obtained has  $\beta$ -5 structure and high antioxidant activity. Ye (2017) used isoeugenol as raw material to synthesize a lignin model compound, confirming that the formation of the  $\beta$ -5 structure enhances its antibacterial properties. Chen (2019) used laccase to catalyze the dehydrogenation polymerization of coniferin to generate DHP. The phenylcoumaran structures in the purified compounds have higher antioxidant, antibacterial, and antitumor activities than the other compounds. Wei (2022) used medium-pressure liquid chromatography to purify guaiacyl-type DHP and determined the physiological activities of the compound obtained, which verifies that the coniferyl aldehyde dimer linked through  $\beta$ -5 structure increases its anticancer activity.

In this study, HRMS and  $^{13}$ C-NMR spectra were used to characterize the structures of the purified compounds L2 and T1 from the two DHPs. The  $\beta$ -5 structures of the L2 and T1 compounds were determined, and both have  $^{13}$ C-NMR signals from C $\alpha$  and C $\beta$  in the  $\beta$ -5 structure. Physiological activity analyses showed that compound L2 had a higher inhibitory effect on HepG2 liver cancer cells than the compound T1, indicating that the carboxyl group in the T1 structure affected the biological activity of the compound. The carboxyl group is polar and can increase the solubility of the compound, meanwhile, an

increase in polarity also reduces its permeability in the lipid membrane. In addition, compounds with a carboxyl structure will form hydrogen or ionic bonds with specific biomolecule portions e.g., enzyme active sites or receptor binding sites, which will also reduce the affinity with their targets. This can indirectly explain why the purified compound T1 exhibited lower biological activity than compound L2. The results of HRMS and  $^{13}$ C-NMR showed that L2 was a lignin dimer with  $\beta$ -5 structure ( $\beta$ -5,  $\gamma$ -CH3, and  $\gamma'$ -CH2OH), and T1 was also a lignin dimer with  $\beta$ -5 structure carrying different functional groups ( $\beta$ -5,  $\gamma$ -CHO, and  $\gamma'$ -COOH). The  $\beta$ -5 structure was the main biologically active substructure in DHPs.

In summary, the lignin-like oligomers had been prepared by dehydrogenation polymerization of coniferin, followed by fractionating with different solvents and purifying with column chromatography. Therefore, the process prevented the secondary condensation reactions that typically arise during the degradation of natural larger lignin molecules. The resulting lignin dimers had  $\beta$ -5 substructure and showed high antitumor activity.

#### **CONCLUSIONS**

- 1. The lignin-like compounds ZL-DHP and ZT-DHP were synthesized through dehydrogenation polymerization of coniferin catalyzed by horseradish peroxidase (HRP), glucose oxidase, and  $\beta$ -glucosidase using the bulk and drop-wise methods, and the yields were 41.9% and 43.3%, respectively. The <sup>13</sup>C-NMR results showed that the two DHPs were very similar to the structure of natural lignin, mainly including  $\beta$ -5,  $\beta$ -O-4,  $\beta$ -1, and  $\beta$ - $\beta$ , and the content of  $\beta$ -5 structure in ZL-DHP was slightly higher than that in ZT-DHP.
- 2. Using organic solvents of different polarities (cyclohexane, ether, ethanol, and dioxane), ZL-DHP and ZT-DHP were graded using the solvent extraction method, and eight graded fractions were obtained: *i.e.*, ZL-1/ZT-1, ZL-2/ZT-2, ZL-3/ZT-3, and ZL-4/ZT-4. In the antitumor assay, ZL-2 and ZT-2 had a significant inhibitory effect on HepG2 cells, with IC<sub>50</sub> 181.99 μg/mL and 246.76 μg/mL, respectively.
- 3. Twelve purified compounds, L1–L6 and T1–T6, with high biological activity were obtained through elution from the ether-soluble components ZL-2 and ZT-2. The IC<sub>50</sub> of L2 and T1 tested for antitumor activity were 33.99 µg/mL and 42.08 µg/mL, respectively. The determination of compound L2 and T1 through HRMS and  $^{13}$ C-NMR revealed that L2 is a lignin dimer with  $\beta$ -5 connection ( $\beta$ -5,  $\gamma$ -CH<sub>3</sub>, and  $\gamma$ '-CH<sub>2</sub>OH), and T1 is also a lignin dimer with  $\beta$ -5 connection but different substituents ( $\beta$ -5,  $\gamma$ -CHO, and  $\gamma$ '-COOH). The  $\beta$ -5 structure was the main biologically active connection mode in DHPs.

#### REFERENCES CITED

Ahamed, M., Ali, D., Alhadlaq, H. A., and Akhtar, M. J. (2013). "Nickel oxide nanoparticles exert cytotoxicity via oxidative stress and induce apoptotic response in human liver cells (HepG2)," *Chemosphere* 93(10), 2514-2522. DOI: 10.1016/j.chemosphere.2013.09.047

- Aljawish, A., Chevalot, I., Jasniewski, J., Paris, C., Scher, J., and Muniglia, L. (2014). "Laccase-catalysed oxidation of ferulic acid and ethyl ferulate in aqueous medium: A green procedure for the synthesis of new compounds," *Food Chemistry* 145, 1046-1054. DOI: 10.1016/j.foodchem.2013.07.119
- Anwanwan, D., Singh, S. K., Singh, S., Saikam, V., and Singh, R. (2020). "Challenges in liver cancer and possible treatment approaches," *Biochimica et Biophysica Acta* (*BBA*) *Reviews on Cancer* 1873(1), 188314. DOI: 10.1016/j.bbcan.2019.188314
- Bele, A. A., and Khale, A. (2011). "An overview on thin layer chromatography," *International Journal of Pharmaceutical Sciences and Research* 2(2), 256.
- Cathala, B., and Monties, B. (2001). "Influence of pectins on the solubility and the molar mass distribution of dehydrogenative polymers (DHPs, lignin model compounds)," *International Journal of Biological Macromolecules* 29(1), 45-51. DOI: 10.1016/S0141-8130(01)00145-3
- Chen, X. (2019). Synthesis and Biological Activity of DHP with Low Degree of Polymerization, Master's Thesis, Hu Bei University of Technology, Wuhan, China.
- Cui, C., Chen, X., Liu, C., Zhu, Y., Zhu, L., Ouyang, J., Shen, Y., Zhou, Z., and Qi, F. (2021). "In situ reactor-integrated electrospray ionization mass spectrometry for heterogeneous catalytic reactions and its application in the process analysis of high-pressure liquid-phase lignin depolymerization," *Analytical Chemistry* 93(38), 12987-12994. DOI: 10.1021/acs.analchem.1c02710
- Dean, K. R., Novak, B., Moradipour, M., Tong, X., Moldovan, D., Knutson, B. L., Rankin, S. E., and Lynn, B. C. (2022). "Complexation of lignin dimers with β-cyclodextrin and binding stability analysis by ESI-MS, isothermal titration calorimetry, and molecular dynamics simulations," *The Journal of Physical Chemistry B* 126(8), 1655-1667. DOI: 10.1021/acs.jpcb.1c09190
- De Castro, M. L., and Priego-Capote, F. (2010). "Soxhlet extraction: Past and present panacea," *Journal of Chromatography A* 1217(16), 2383-2389. DOI: 10.1016/j.chroma.2009.11.027
- Freudenberg, K. (1965). "Lignin: Its constitution and formation from p-hydroxycinnamyl alcohol: Lignin is duplicated by dehydrogenation of these alcohols; intermediates explain formation and structure," *Science* 148(3670), 595-600.
- Johjima, T., Itoh, N., Kabuto, M., Tokimura, F., Nakagawa, T., Wariishi, H., and Tanaka, H. (1999). "Direct interaction of lignin and lignin peroxidase from *Phanerochaete chrysosporium*," *Proceedings of the National Academy of Sciences* 96(5), 1989-1994. DOI: 10.1073/pnas.96.5.1989
- Kumar, P., Nagarajan, A., and Uchil, P. D. (2018). "Analysis of cell viability by the MTT assay," Cold spring harbor protocols 2018(6), pdb. prot095505. DOI: 10.1101/pdb.prot095505
- Liu, H., Pei, J., Hu, H., and Pei, Y. (2010). "Spectra analysis of lignin small molecular guaiacyl coniferyl alcohol biological modification treated by laccase," *Guang Pu Xue Yu Guang Pu Fen Xi* 30(6), 1469-1473. DOI: 10.3964/j.issn.1000-0593(2010)06-1469-05
- Liu, J., Shen, H., and Ong, C. (2000). "Salvia miltiorrhiza inhibits cell growth and induces apoptosis in human hepatoma HepG2 cells," Cancer Letters 153(1-2), 85-93. DOI: 10.1016/s0304-3835(00)00391-8
- Long, J.-L., Zhu, Q.-J., Bai, J., et al. (2021). "Optimization of the process of producing antioxidant peptides from *Aspergillus oryzae* solid-state fermentation Perilla seed meal," *Journal of Light Industry* 36(4), DOI: 10.12187/2021.04.003

- Matsushita, Y., Ko, C., Aoki, D., Hashigaya, S., Yagami, S., and Fukushima, K. (2015). "Enzymatic dehydrogenative polymerization of monolignol dimers," *Journal of Wood Science* 61608-61619. DOI: 10.1007/s10086-015-1513-8
- Mattinen, M., Maijala, P., Nousiainen, P., Smeds, A., Kontro, J., Sipilä, J., Tamminen, T., Willför, S., and Viikari, L. (2011). "Oxidation of lignans and lignin model compounds by laccase in aqueous solvent systems," *Journal of Molecular Catalysis B: Enzymatic* 72(3-4), 122-129. DOI: 10.1016/j.molcatb.2011.05.009
- Méchin, V., Baumberger, S., Pollet, B., and Lapierre, C. (2007). "Peroxidase activity can dictate the *in vitro* lignin dehydrogenative polymer structure," *Phytochemistry* 68(4), 571-579. DOI: 10.1016/j.phytochem.2006.11.024
- Nga, N., Ngoc, T., Trinh, N., Thuoc, T. L., and Thao, D. (2020). "Optimization and application of MTT assay in determining density of suspension cells," *Analytical Biochemistry* 610113937. DOI: 10.1016/j.ab.2020.113937
- Park, S., Ang, R. R., Duffy, S. P., Bazov, J., Chi, K. N., Black, P. C., and Ma, H. (2014). "Morphological differences between circulating tumor cells from prostate cancer patients and cultured prostate cancer cells," *PloS One* 9(1), article e85264. DOI: 10.1371/journal.pone.0085264
- Sheng, H., Tang, W., Gao, J., Riedeman, J. S., Li, G., Jarrell, T. M., Hurt, M. R., Yang, L., Murria, P., and Ma, X. (2017). "(–) ESI/CAD MS n procedure for sequencing lignin oligomers based on a study of synthetic model compounds with β-O-4 and 5-5 linkages," *Analytical Chemistry* 89(24), 13089-13096. DOI: 10.1021/acs.analchem.7b01911
- Shu, F., Jiang, B., Yuan, Y., Li, M., Wu, W., Jin, Y., and Xiao, H. (2021). "Biological activities and emerging roles of lignin and lignin-based products— A review," *Biomacromolecules* 22(12), 4905-4918. DOI: 10.1021/acs.biomac.1c00805
- Takahashi, L. K., Zhou, J., Kostko, O., Golan, A., Leone, S. R., and Ahmed, M. (2011). "Vacuum-ultraviolet photoionization and mass spectrometric characterization of lignin monomers coniferyl and sinapyl alcohols," *The Journal of Physical Chemistry A* 115(15), 3279-3290. DOI: 10.1021/jp111437e
- Terashima, N., Atalla, R. H., Ralph, S. A., *et al.* (1995). "New preparations of lignin polymer models under conditions that approximate cell wall lignification. I. Synthesis of novel lignin polymer models and their structural characterization by 13 C NMR," *Holzforschung* 49, 521-527.
- Terashima, N., Atalla, R. H., Ralph, S. A., *et al.* (1996). "New preparations of lignin polymer models under conditions that approximate cell wall lignification. II. Structural characterization of the models by thioacidolysis," *Holzforschung* 50, 9-14.
- Tobimatsu, Y., Takano, T., Kamitakahara, H., and Nakatsubo, F. (2006). "Studies on the dehydrogenative polymerizations of monolignol β-glycosides. Part 2: Horseradish peroxidase-catalyzed dehydrogenative polymerization of isoconiferin," *Holzforschung* 60(5). DOI: 10.1515/hf.2006.085
- Ugartondo, V., Mitjans, M., and Vinardell, M. P. (2008). "Comparative antioxidant and cytotoxic effects of lignins from different sources," *Bioresource Technology* 99(14), 6683-6687.
- Van Meerloo, J., Kaspers, G. J., and Cloos, J. (2011). "Cell sensitivity assays: The MTT assay," in: *Cancer Cell Culture: Methods and Protocols*, Humana Press, Totowa, NJ, USA, pp. 237-245. DOI: 10.1007/978-1-61779-080-5 20
- Wang, Y., Zhu, R., and Chen, H. (2006). "Thin-layer chromatography and its progress," *University Chemistry* (03), 34-40.

- Wei, X. (2022). *Preparation and Antitumor Activity of G-DHP and Ginkgo Kraft Lignin*, Master's Thesis, Hu Bei University of Technology, Wuhan, China.
- Xie, Y.-M., Yasuda, S., Wu, H., and Liu, H.-B. (1994). "Selective carbon 13 enrichment of side chain carbons of ginkgo lignin traced by carbon 13 nuclear magnetic resonance," *Plant Physiology and Biochemistry* 32, 243-249.
- Xie, Y., Jiang, C., Chen, X., Wu, H., and Bi, S. (2020). "Preparation of oligomeric phenolic compounds (DHPs) from coniferin and syringin and characterization of their anticancer properties," *BioResources* 15(1), 1791-1809. DOI: 10.15376/biores.15.1.1791-1809
- Ye, Z. (2017). Research on the Synthesis of Lignin Oligomers in vitro and Their Biological Activities, Master's Thesis, Hu Bei University of Technology, Wuhan, China
- Yue, F., Lu, F., Ralph, S., and Ralph, J. (2016). "Identification of 4–O–5-units in softwood lignins via definitive lignin models and NMR," *Biomacromolecules* 17(6), 1909-1920. DOI: 10.1021/acs.biomac.6b00256
- Zega, A., Srčič, S., Mavri, J., and Bešter-Rogač, M. (2008). "Molecular interactions of 1, 4-dihydropyridine derivatives with selected organic solvents: A volumetric, spectroscopic and computational study," *Journal of Molecular Structure* 875(1-3), 354-363.
- Zhang, B., Li, L., Li, Z., Liu, Y., Zhang, H., and Wang, J. (2016). "Carbon ion-irradiated hepatoma cells exhibit coupling interplay between apoptotic signaling and morphological and mechanical remodeling," *Scientific Reports* 6(1), 35131. DOI: 10.1038/srep35131
- Zhang, R., Qi, Y., Ma, C., Ge, J., Hu, Q., Yue, F., Li, S., and Volmer, D. (2021). "Characterization of lignin compounds at the molecular level," *Molecules* 26(1). DOI: 10.18452/22494
- Zhao, H., Feng, Q., Xie, Y., Li, J., and Chen, X. (2017). "Preparation of biocompatible hydrogel from lignin-carbohydrate complex (LCC) as cell carriers," *BioResources* 12(4), 8490-8504.
- Zhou, J., Yue, Y., Wei, X., and Xie, Y. (2023). "Preparation and anti-lung cancer activity analysis of guaiacyl-type dehydrogenation polymer," *Molecules* 28(8), 3589. DOI: 10.3390/molecules28083589

Article submitted: November 18, 2024; Peer review completed: January 4, 2025; Revised version received: January 23, 2025; Accepted: January 26, 2025; Published: February 25, 2025

DOI: 10.15376/biores.20.2.2904-2921